

# In Situ and Reactor Study of the Enantioselective Hydrogenation of Acetylacetone by Ruthenium Catalysis with the New Chiral Diphosphine Ligand (*R*)-(*R*)-3-Benzyl-2,4-bis(diphenylphosphino)pentane

Claudio Bianchini,<sup>\*,†</sup> Pierluigi Barbaro, Giancarlo Scapacci, and Fabrizio Zanolini

*Istituto per lo Studio della Stereochimica ed Energetica dei Composti di Coordinazione, ISSECC-CNR, Via J. Nardi 39, I-50132 Firenze, Italy*

Received February 14, 2000

The new optically pure  $C_1$ -symmetric diphosphine ligand (*R*)-(*R*)-3-benzyl-2,4-bis(diphenylphosphino)pentane (BDPBzP) has been synthesized by enantioselective reduction of 3-benzyl-2,4-pentanedione with [(*S*)-BINAP]Ru(*p*-cymene)Cl]Cl, followed by the reaction of potassium diphenylphosphide with the bis(mesylate) intermediate (*S*)-(*S*)-PhCH<sub>2</sub>CH(CH(OMs)CH<sub>3</sub>)<sub>2</sub>. The Ru(II) complexes [(BDPBzP)Ru(*p*-cymene)I]I·2CH<sub>2</sub>Cl<sub>2</sub> (**5**), [(BDPBzP)-(DMSO)Ru( $\mu$ -Cl)<sub>3</sub>RuCl(BDPBzP)] (**6a**), and [(BDPBzP)RuCl(CH<sub>3</sub>CN)<sub>3</sub>]OTf (**7**) have been prepared and characterized by multinuclear NMR spectroscopy. The *p*-cymene complex **5** has been authenticated by a single-crystal X-ray analysis. All Ru(II) complexes are effective catalyst precursors for the enantioselective hydrogenation of acetylacetone to (*R*)-(*R*)-2,4-pentanediol. The best catalytic performance in terms of enantioselective discrimination (ee's up to 99%) has been observed for the dimer **6a**. An in situ high-pressure NMR study in catalytic conditions has shown that the nonclassical polyhydride dimer [(BDPBzP)( $\eta^2$ -H<sub>2</sub>)ClRu( $\mu$ -H)<sub>2</sub>RuCl( $\eta^2$ -H<sub>2</sub>)(BDPBzP)] is the only species observed all over the catalytic cycle. The monohydrogenated intermediate (*R*)-4-hydroxypentan-2-one is obtained in appreciable yields only at low temperature or low conversion. The relative yields and ee's of the mono- and dihydrogenated products are consistent with the effect of a double stereodifferentiation process.

## Introduction

Enantioselective catalysis has reached an important level of broad applicability, and many highly selective methods are currently employed to obtain optically pure intermediates used in fine chemicals industry.  $C_2$ -symmetric bidentate phosphine ligands have largely contributed to this success in combination with various transition metal ions.<sup>1</sup> As compared to monophosphines,  $C_2$ -symmetric diphosphines are actually endowed with superior properties in asymmetric catalysis for their capability to restrict the number of competing asymmetric conformations surrounding a metal center. In particular, it is a commonly held belief that the performance of  $C_2$ -symmetric diphosphine ligands is governed by both the induction influence of the chelate ring and the backbone flexibility.<sup>1</sup>

Based on an alternative view of the stereodifferentiation properties of chiral catalysts,<sup>2</sup> the design of chiral

dissymmetric diphosphine ligands is now receiving increasing attention. The concept developed by Achiwa et al. is that intermediates in some catalytic cycles may lack the intrinsic symmetry of the ligand, and therefore, in such cases,  $C_1$ -symmetric diphosphines may provide better results than  $C_2$ -symmetric diphosphines.<sup>2</sup> Indeed, a number of successful asymmetric reactions accomplished by catalysts containing dissymmetric diphosphine ligands have been reported.<sup>2,3</sup>

In this paper, we describe the synthesis of the new optically pure diphosphine (*R*)-(*R*)-3-benzyl-2,4-bis(diphenylphosphino)pentane (BDPBzP), which differs from the well-known  $C_2$ -symmetric counterpart BDPP for the presence of a benzyl group at the  $C_2$ -position of the ligand backbone. Besides removing the  $C_2$ -symmetry, the introduction of the benzyl substituent reduces the ligand flexibility<sup>4</sup> with a potential positive effect on asymmetric induction.<sup>2,5</sup>

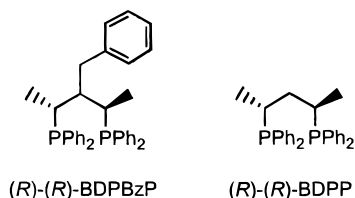
The BDPBzP ligand has been employed to synthesize both mononuclear and dinuclear ruthenium(II) complexes whose catalytic performance in the enantioselective hydrogenation of acetylacetone to (*R*)-(*R*)-2,4-

<sup>†</sup> E-mail: bianchin@fi.cnr.it.

(1) (a) Brown, J. M. *Chem. Soc. Rev.* **1993**, 22, 25. (b) Brunner, H.; Zettlmeier, W. *Handbook of Enantioselective Catalysis with Transition Metal Compounds*; VCH: Weinheim, 1993; Vols. 1, 2. (c) Whitesell, J. K. *Chem. Rev.* **1989**, 89, 1581. (d) Kagan, H. B. In *Asymmetric Synthesis*; Morrison, J. D., Ed.; Academic Press: Orlando, FL, 1985; Vol. 5, pp 1–35, and references therein.

(2) (a) Inoguchi, K.; Sakuraba, S.; Achiwa, K. *Synlett* **1992**, 169. (b) Morimoto, T.; Chiba, M.; Achiwa, K. *Chem. Pharm. Bull.* **1993**, 41, 1149. (c) RajanBabu, T. V.; Casalnuovo, A. L. *J. Am. Chem. Soc.* **1996**, 118, 6325.

(3) (a) Carmichael, D.; Doucet, H.; Brown, J. M. *J. Chem. Soc., Chem. Commun.* **1999**, 261. (b) Casey, C. P.; Paulsen, E. L.; Beuttenmueller, E. W.; Proft, B. R.; Matter, B. A.; Powell, D. R. *J. Am. Chem. Soc.* **1999**, 121, 63. (c) Gleich, D.; Herrmann, W. A. *Organometallics* **1999**, 18, 4354.



pentanediol has been studied in standard autoclaves. In addition to this investigation, the hydrogenation of acetylacetone with a representative Ru BDPBzP catalyst has been studied in situ by high-pressure NMR (HPNMR) spectroscopy. Indeed, this technique allows one to study a reaction at elevated gas pressure in experimental conditions that are very much similar to those of actual reactor conditions.<sup>6</sup> Obviously, the HPNMR technique provides a picture of what can be seen by NMR spectroscopy in terms of concentration, lifetime, magnetic relaxation, and dynamics of the chemical species involved in the process under investigation. Nevertheless, many successful applications of HPNMR spectroscopy to homogeneous catalysis have recently been reported, and some of them have largely contributed to solve intriguing mechanistic issues.<sup>6d-n</sup>

The most interesting result produced by the HPNMR investigation is the observation of a dimeric nonclassical polyhydrido Ru(II) complex all over the reduction of acetylacetone, which represents a novelty in catalytic hydrogenation reactions.

## Experimental Section

**General Information.** All reactions and manipulations were performed under a pure nitrogen atmosphere unless otherwise stated. Freshly distilled, dry solvents were used throughout. [Ru(*p*-cymene)I<sub>2</sub>]<sub>2</sub><sup>7</sup> and RuCl<sub>2</sub>(DMSO)<sub>4</sub><sup>8</sup> were synthesized as previously reported. [(*S*)-BINAP]Ru(*p*-cymene)-Cl]Cl was obtained from Aldrich. All the other chemicals were commercial products and were used as received without further purification. The solid compounds were collected on sintered glass frits before being dried in a stream of nitrogen. <sup>31</sup>P{<sup>1</sup>H} NMR spectra were recorded on either a Bruker 200-

ACP spectrometer operating at 81.01 MHz or a Bruker Avance DRX-500 spectrometer operating at 202.46 MHz. Chemical shifts are relative to external 85% H<sub>3</sub>PO<sub>4</sub> with downfield values reported as positive. <sup>1</sup>H and <sup>13</sup>C{<sup>1</sup>H} NMR spectra were recorded at 200.13 and 50.32 MHz, respectively, on a Bruker 200-ACP spectrometer or at 500.13 and 125.76 MHz, respectively, on a Bruker Avance DRX-500 spectrometer. Chemical shifts are relative to tetramethylsilane as external reference or calibrated against solvent resonances. The assignments of the signals resulted from <sup>1</sup>H homonuclear decoupling experiments, <sup>1</sup>H COSY, <sup>1</sup>H NOESY, and proton detected <sup>1</sup>H-<sup>13</sup>C and <sup>1</sup>H-<sup>31</sup>P correlations using degassed nonspinning samples. 2D NMR spectra were recorded on a Bruker Avance DRX-500 spectrometer using pulse sequences suitable for phase-sensitive representations using TPPI. The <sup>1</sup>H-<sup>13</sup>C correlations<sup>9</sup> and <sup>1</sup>H-<sup>31</sup>P correlations<sup>10</sup> were recorded using the standard HMQC sequence with no decoupling during acquisition. <sup>1</sup>H NOESY<sup>11</sup> spectra were acquired with 1024 increments of size 2K covering the full range in both dimensions with a mixing time of 800 ms. <sup>1</sup>H and <sup>1</sup>H{<sup>31</sup>P} NMR experiments carried out in CH<sub>3</sub>OH solution were recorded at 500.132 MHz using a Watergate sequence for the minimization of solvent signal.<sup>12,13</sup> Coupling constants were obtained by computer simulation. *T*<sub>1</sub> measurements were performed with the inversion-recovery method using a modified pulse sequence allowing the presaturation of solvent resonances.<sup>14</sup> The high-pressure NMR experiments were performed with a titanium high-pressure charging head constructed at the ISSECC-CNR,<sup>15</sup> while the 10 mm sapphire NMR tube was purchased from Saphikon, Milford, NH. *Note:* Since high gas pressures are involved, safety precautions must be taken at all stages of studies involving high-pressure NMR tubes. Infrared spectra were recorded on a Perkin-Elmer 1600 Series FT-IR spectrometer using samples milled in Nujol between KBr plates. Merck silica gel 60, 230–400 mesh ASTM, was used for column chromatography. Thin-layer chromatography was performed with Macherey-Nagel Polygram SIL G/UV254 precoated plastic sheets. Reactions under a controlled pressure of hydrogen were performed with a stainless steel autoclave (100 mL internal volume) constructed at ISSECC-CNR (Firenze, Italy) and equipped with a magnetic stirrer, a glass inset, and a pressure controller. The temperature control was achieved by an oil bath thermostat accurate to ±0.2 °C. GC analyses were performed either on a Shimadzu GC-14A gas chromatograph equipped with a flame ionization detector and a 30 m (0.25 mm i.d., 0.25 μm FT) SPB-1 Supelco fused silica capillary column and coupled with a C-R6A Chromatopac operating in the corrected area method or with a Shimadzu GC-17A gas chromatograph equipped with a flame ionization detector and a 40 m × 0.25 mm i.d. Chiraldex G-TA capillary column and coupled with a Shimadzu C-R7A Chromatopac. GC/MS analyses were performed on a Shimadzu QP 2000 apparatus equipped with a column identical to that used for GC analyses (SPB-1). The organic compounds were identified by their GC/MS spectra. HPLC analyses were performed with a Shimadzu LC-8A liquid chromatograph coupled with a Shimadzu SPD-M6A photodiode array UV–vis detector operating in the 200–350 nm wavelength range and equipped with a Daicel Chiralcel OD-H 0.46 × 25 cm column. Optical rotations were measured with a Perkin-Elmer 341 polarimeter using 10 cm cells.

(9) Summers, M. F.; Marzilli, L. G.; Bax, A. *J. Am. Chem. Soc.* **1986**, *108*, 4285.

(10) Jeener, J.; Meier, G. H.; Bachmann, P.; Ernst, R. *J. Chem. Phys.* **1979**, *71*, 4545.

(11) Sklenar, V.; Miyashiro, H.; Zon, G.; Miles, H. T.; Bax, A. *FEBS Lett.* **1986**, *208*, 94.

(12) Piotto, M.; Saudek, V.; Sklenar, V. *J. Biomol. NMR* **1992**, *2*, 661.

(13) Sklenar, V.; Piotto, M.; Leppik, R.; Saudek, V. *J. Magn. Reson.* **1993**, *102*, 241.

(14) Guéron, M.; Plateau, P.; Decors, M. *Prog. NMR Spectrosc.* **1991**, *23*, 135.

(15) Bianchini, C.; Meli, A.; Traversi, A. IT, FI97 A000025 1997.

(4) (a) Doherty, S.; Eastham, G. R.; Tooze, R. P.; Scanlan, T. H.; Williams, D.; Elsegood, M. R. J.; Clegg, W. *Organometallics* **1999**, *18*, 3558. (b) Bianchini, C.; Lee, H. M.; Meli, A.; Moneti, S.; Vizza, F.; Fontani, M.; Zanello, P. *Macromolecules* **1999**, *32*, 4183. (c) Bianchini, C.; Lee, H. M.; Barbaro, P.; Meli, A.; Moneti, S.; Vizza, F. *New J. Chem.* **1999**, *23*, 929.

(5) Marinetti, A.; Genet, J.-P.; Jus, S.; Blanc, D.; Ratevelomanana-Vidal, V. *Chem. Eur. J.* **1999**, *5*, 1160.

(6) (a) Horváth, I. T.; Millar, J. M. *Chem. Rev.* **1991**, *91*, 1339. (b) Elsevier, C. J. *J. Mol. Catal.* **1994**, *92*, 285. (c) Roe, D. C. *J. Magn. Reson.* **1985**, *63*, 388. (d) Bianchini, C.; Frediani, P.; Meli, A.; Peruzzini, M.; Vizza, F. *Chem. Ber.* **1997**, *130*, 1633. (e) Bianchini, C.; Herrera, V.; Jiménez, M. V.; Meli, A.; Sánchez-Delgado, R. A.; Vizza, F. *J. Am. Chem. Soc.* **1995**, *117*, 8567. (f) Bianchini, C.; Fabbri, D.; Gladiali, S.; Meli, A.; Pohl, W.; Vizza, F. *Organometallics* **1996**, *15*, 4604. (g) Bianchini, C.; Casares, J. A.; Meli, A.; Sernau, V.; Vizza, F.; Sánchez-Delgado, R. A. *Polyhedron* **1997**, *16*, 3099. (h) Bianchini, C.; Meli, A.; Patinec, V.; Sernau, V.; Vizza, F. *J. Am. Chem. Soc.* **1997**, *119*, 4945. (i) Bianchini, C.; Meli, A.; Moneti, S.; Vizza, F. *Organometallics* **1998**, *17*, 2636. (j) Bianchini, C.; Lee, H. M.; Meli, A.; Moneti, M.; Patinec, V.; Petrucci, G.; Vizza, F. *Macromolecules* **1999**, *32*, 3859. (k) Bianchini, C.; Meli, A.; Moneti, S.; Oberhauser, W.; Vizza, F.; Herrera, V.; Fuentes, A.; Sánchez-Delgado, R. A. *J. Am. Chem. Soc.* **1999**, *121*, 7071. (l) Bianchini, C.; Lee, H. M.; Meli, A.; Vizza, F. *Organometallics* **2000**, *33*, XX. (m) Moore, K. T.; Horváth, I. T.; Therien, M. J. *J. Am. Chem. Soc.* **1997**, *119*, 1791. (n) Horváth, I. T.; Kastrup, R. V.; Oswald, A. A.; Mozeleski, E. J. *Catal. Lett.* **1989**, *2*, 85.

(7) Mashima, K.; Kusano, K.; Ohta, T.; Noyori, R.; Takaya, H. *J. Chem. Soc., Chem. Commun.* **1989**, 1208.

(8) James, B. R.; Ochiai, E.; Rempel, G. I. *Inorg. Nucl. Chem. Lett.* **1971**, *7*, 701.



**Synthesis of the Chiral Ligand (*R*)-(*R*)-PhCH<sub>2</sub>CH(CH<sub>2</sub>PPh<sub>2</sub>)CH<sub>2</sub>CH<sub>2</sub>COCH<sub>3</sub> (**1**).** A solution of 2,4-pentanedione (25.0 g, 0.25 mol) in dry ethanol (30 mL) was added dropwise to a solution of sodium (5.8 g, 0.25 mol) in dry ethanol (180 mL). The resulting mixture was stirred at room temperature for 30 min. Then a solution of benzyl bromide (42.7 g, 0.25 mol) in dry ethanol (30 mL) was added at room temperature. After refluxing for 2 h, the mixture was cooled to room temperature and KBr was filtered off. The solvent was removed in vacuo, and the oil obtained was distilled twice (bp<sub>25</sub> 215 °C) to give pure **1** in 88% yield as a colorless liquid. Anal. Calcd for C<sub>12</sub>H<sub>14</sub>O<sub>2</sub>: C, 75.76; H, 7.42. Found: C, 75.70; H, 7.51. <sup>1</sup>H NMR (CDCl<sub>3</sub>, 294 K, 200.13 MHz): 7.1–7.4 (m, 5H, Ph), 4.03 (t, 1H, CH, *J* = 8.1 Hz), 3.18 (d, 2H, CH<sub>2</sub>), 2.12 (d, 6H, CH<sub>3</sub>).

**(*S*)-(*S*)-PhCH<sub>2</sub>CH(CH(OH)CH<sub>3</sub>)CH<sub>2</sub>CH<sub>2</sub>COCH<sub>3</sub> (**2**).** The reduction of the diketone **1** was accomplished using [(*S*)-BINAP]Ru(*p*-cymene)-Cl]Cl as chiral catalyst.<sup>16</sup> A solution of **1** (15.0 g, 0.08 mol) and the catalyst (0.2 mmol) in EtOH (50 mL) was introduced into a stainless steel autoclave under nitrogen. The autoclave was then filled with 70 atm H<sub>2</sub> and the mixture stirred at room temperature for 48 h. The ethanol solvent was removed in vacuo, and the solid obtained was recrystallized twice from diethyl ether/*n*-hexane. Compound **2** was obtained as an ivory crystalline solid in 88% yield. Anal. Calcd for C<sub>12</sub>H<sub>18</sub>O<sub>2</sub>: C, 74.19; H, 9.34. Found: C, 74.28; H, 9.25. <sup>1</sup>H NMR (CDCl<sub>3</sub>, 294 K, 200.13 MHz): 7.1–7.4 (m, 5H, Ph), 4.28 (qd, 1H, CH<sub>3</sub>C'H, *J* = 6.4, *J* = 2.8 Hz), 3.94 (qd, 1H, CH<sub>3</sub>C''H, *J* = 6.1, *J* = 4.0 Hz), 2.83 (dd, 1H, CHH, *J* = 14.0, *J* = 8.9 Hz), 2.69 (dd, 1H, CHH, *J* = 14.0, *J* = 6.2 Hz), 1.69 (m, 1H, CH), 1.31 (d, 3H, CH<sub>3</sub>C'), 1.27 (d, 3H, CH<sub>3</sub>C''). [α]<sub>D</sub><sup>25</sup> = −28.9 (*c* = 1.8, CHCl<sub>3</sub>). <sup>1</sup>H NMR analysis proved the *de* and *ee* (using the shift reagent (S)-(+)-2,2,2-trifluoro-1-(9-anthryl)ethanol) of the isolated product to be 100% and 98%, respectively.

**(*S*)-(*S*)-PhCH<sub>2</sub>CH(CH(OMs)CH<sub>3</sub>)CH<sub>2</sub>CH<sub>2</sub>COCH<sub>3</sub> (**3**).** Methanesulfonyl chloride (3.2 mL, 40 mmol) was added dropwise at 0 °C over a 30 min period to a solution of **2** (2.50 g, 13 mmol) in dry pyridine (20 mL) with stirring. The resulting mixture was stored at 0 °C for 24 h. Cold water (50 mL) was then added at 0 °C, to give a viscous oil, which was washed twice with water (50 mL). The solid obtained was recrystallized twice from ethanol. Yield: 81.2%. Anal. Calcd for C<sub>14</sub>H<sub>22</sub>O<sub>6</sub>S<sub>2</sub>: C, 47.98; H, 6.33. Found: C, 48.28; H, 6.39. <sup>1</sup>H NMR (CDCl<sub>3</sub>, 294 K, 200.13 MHz): 7.2–7.4 (m, 5H, Ph), 5.12 (qd, 1H, CH<sub>3</sub>C'H, *J* = 6.6, *J* = 2.8 Hz), 4.97 (qd, 1H, CH<sub>3</sub>C''H, *J* = 6.5, *J* = 4.9 Hz), 3.08 (s, 3H, OCH<sub>3</sub>'), 3.04 (s, 3H, OCH<sub>3</sub>''), 2.90 (dd, 1H, CHH, *J* = 14.8, *J* = 6.2 Hz), 2.82 (dd, 1H, CHH, *J* = 14.8, *J* = 7.4 Hz), 2.26 (m, 1H, CH), 1.54 (d, 3H, CH<sub>3</sub>C'), 1.52 (d, 3H, CH<sub>3</sub>C''). Mp: 71–73 °C. [α]<sub>D</sub><sup>25</sup> = −35.5 (*c* = 2.1, CHCl<sub>3</sub>).

**BDPBzP (**4**).** A solution of **3** (1.75 g, 5.0 mmol) in dry THF (20 mL) was added dropwise at 0 °C to a solution of KPh<sub>2</sub>·2dioxane (4.0 g, 10 mmol) in dry THF (40 mL) under stirring over a period of 30 min, causing a color change from red to light yellow. The mixture was allowed to react for 3 h at room temperature, and the solvent was then removed in vacuo. The residue obtained was dissolved in diethyl ether (30 mL) and added to a solution of Ni(NCS)<sub>2</sub> (0.87 g, 5.0 mmol) in EtOH (15 mL) under stirring. Pure BDPBzP was obtained by isolation of its Ni(II) thiocyanate complex, followed by cyanolysis with KCN.<sup>17,18</sup> Yield: 63.0%. Mp: 93–95 °C. Anal. Calcd for C<sub>36</sub>H<sub>36</sub>P<sub>2</sub>: C, 81.48; H, 6.84. Found: C, 81.29; H, 6.85. [α]<sub>D</sub><sup>25</sup> = +84.7 (*c* = 3.8, CHCl<sub>3</sub>). <sup>1</sup>H NMR analysis showed the compound to be diastereomerically pure. The enantiomeric purity was checked by an NMR-scale test reaction after

conversion to the corresponding phosphine oxide with H<sub>2</sub>O<sub>2</sub> (<sup>31</sup>P NMR, δ 43.5; 34.0 ppm, CDCl<sub>3</sub>) and addition of (−)-*O,O'*-dibenzoyl-L-tartaric acid. No splitting of the <sup>1</sup>H and <sup>31</sup>P{<sup>1</sup>H} resonances was observed.

**[(BDPBzP)Ru(*p*-cymene)]I<sub>2</sub>·2CH<sub>2</sub>Cl<sub>2</sub> (**5**).** A mixture of BDPBzP (0.20 g, 0.38 mmol) and [Ru(*p*-cymene)I<sub>2</sub>]<sub>2</sub> (0.18 g, 0.19 mmol) in 4:1 (v/v) CH<sub>2</sub>Cl<sub>2</sub>/methanol (10 mL) was refluxed with stirring for 1 h. After the flask was cooled to room temperature, diethyl ether (20 mL) was added. Slow evaporation of the solvent under a stream of nitrogen gave red crystals of **5** in 77% yield. Anal. Calcd for C<sub>48</sub>H<sub>54</sub>Cl<sub>4</sub>I<sub>2</sub>P<sub>2</sub>Ru: C, 48.46; H, 4.58. Found: C, 48.44; H, 4.63. <sup>1</sup>H NMR (CDCl<sub>3</sub>, 294 K, 200.13 MHz): 7.7–7.8 (m, 3H), 7.4–7.6 (m, 12H), 7.1–7.4 (m, 6H), 6.7–6.9 (m, 4H), 6.10 (s, 2H), 5.62 (dd, 1H), 4.96 (d, 1H), 3.55 (m, 1H), 3.38 (qnt, 1H), 3.05 (m, 1H), 2.69 (m, 1H), 2.43 (m, 2H), 1.35 (dd, 3H), 1.25 (dd, 3H), 1.22 (d, 3H), 0.92 (s, 3H), 0.7 (d, 3H).

**[(BDPBzP)(DMSO)Ru(μ-Cl)<sub>2</sub>RuCl(BDPBzP)] (**6a**).** A mixture of BDPBzP (0.40 g, 0.75 mmol) and RuCl<sub>2</sub>(DMSO)<sub>4</sub> (0.36 g, 0.75 mmol) in ethanol (15 mL) was refluxed with stirring for 2.5 h, causing the separation of a yellow-orange solid. After cooling the solid to room temperature, *n*-pentane (20 mL) was added, and the solid obtained was filtered off and washed with *n*-pentane (50 mL). Yield: 68%. Anal. Calcd for C<sub>74</sub>H<sub>78</sub>Cl<sub>4</sub>OP<sub>4</sub>SRu<sub>2</sub>: C, 59.92; H, 5.30. Found: C, 60.01; H, 5.45. <sup>1</sup>H NMR (C<sub>6</sub>D<sub>6</sub>, 294 K, 500.13 MHz): 3.91 (dqnt, 1H, CH<sub>3</sub>CHP<sup>A</sup>), 3.77 (dqnt, 1H, CH<sub>3</sub>CHP<sup>B</sup>), 3.64 (dqnt, 1H, CH<sub>3</sub>CHP<sup>B</sup>), 3.27 (dqnt, 1H, CH<sub>3</sub>CHP<sup>A</sup>), 2.94 (s, 3H, CH<sub>3</sub>SO), 2.77 (m, 1H, CHH<sup>A</sup>), 2.75 (s, 3H, CH<sub>3</sub>SO), 2.68 (m, 1H, CHH<sup>B</sup>), 2.65 (m, 1H, CH<sup>A</sup>), 2.61 (m, 1H, CH<sup>B</sup>), 2.51 (t, 1H, CHH<sup>A</sup>), 2.44 (t, 1H, CHH<sup>B</sup>), 1.67 (dd, 3H, CH<sub>3</sub>CP<sup>B</sup>), 1.61 (dd, 3H, CH<sub>3</sub>CP<sup>A</sup>), 1.30 (dd, 3H, CH<sub>3</sub>CP<sup>A</sup>), 0.95 (dd, 3H, CH<sub>3</sub>CP<sup>B</sup>). <sup>13</sup>C NMR (C<sub>6</sub>D<sub>6</sub>, 294 K, 125.76 MHz): 52.51 (s, CH<sub>3</sub>SO), 42.42 (s, CH<sup>A</sup>), 41.51 (s, CH<sup>B</sup>), 37.75 (t, CH<sub>2</sub><sup>A</sup>), 37.51 (t, CH<sub>2</sub><sup>B</sup>), 36.50 (d, CH<sub>3</sub>CP<sup>A</sup>), 31.01 (d, CH<sub>3</sub>CP<sup>B</sup>), 26.56 (d, CH<sub>3</sub>CP<sup>A</sup>), 25.38 (d, CH<sub>3</sub>CP<sup>B</sup>), 16.02 (s, CH<sub>3</sub>CP<sup>B</sup>), 15.71 (s, CH<sub>3</sub>CP<sup>A</sup>), 11.83 (s, CH<sub>3</sub>CP<sup>A</sup>), 11.19 (s, CH<sub>3</sub>CP<sup>B</sup>). IR: 1110 ν(S–O) cm<sup>−1</sup>.

**[(BDPBzP)RuCl(CH<sub>3</sub>CN)<sub>3</sub>]OTf (**7**).** A mixture of **6a** (0.17 g, 0.11 mmol) and AgOTf (0.03 g, 0.23 mmol) in CH<sub>3</sub>CN (20 mL) was stirred at room temperature overnight. After AgCl was filtered off, the light yellow solution obtained was concentrated to ca. 3 mL under vacuum. By addition of diethyl ether (20 mL), a yellow oil was obtained, which slowly solidified on standing. The solid compound was filtered off and washed with diethyl ether (100 mL). Yield: 76%. Anal. Calcd for C<sub>43</sub>H<sub>45</sub>N<sub>3</sub>ClF<sub>3</sub>O<sub>3</sub>P<sub>2</sub>SRu: C, 54.98; N, 4.47; H, 4.83. Found: C, 55.07; N, 4.31; H, 4.86. <sup>1</sup>H NMR (CD<sub>2</sub>Cl<sub>2</sub>, 294 K, 200.13 MHz): 6.8–7.8 (m, 25H), 3.40 (bm, 1H), 2.7–3.0 (m, 3H), 2.56 (t, 1H), 2.16 (s, 3H), 1.92 (s, 3H), 1.84 (s, 3H), 1.0–1.2 (m, 6H). IR: 2328, 2314, 2310 ν(C–N) cm<sup>−1</sup>.

**Enantioselective Hydrogenation of Acetylacetone.** In a typical experiment a suspension of the catalyst precursor (0.005 mmol) in ethanol (20 mL) was stirred at 60 °C under argon until the complete dissolution of the starting complex occurred (ca. 30 min). Acetylacetone (0.8 mmol) was added at room temperature, and the resulting solution was transferred via a Teflon capillary into a 100 mL autoclave under argon. Argon was then replaced by hydrogen with three cycles 5 bar/normal pressure. The autoclave was finally charged with the desired pressure of H<sub>2</sub> and then heated using a thermostated oil bath with magnetic stirring. After the desired time, the reactor was cooled to room temperature and a sample of the reaction mixture was analyzed by GC and GC/MS. The absolute configuration of the hydrogenated products was determined by comparison of the observed GC retention times with those of authentic specimens.

**In Situ HPNMR Studies.** A 10 mm sapphire HPNMR tube was charged with **6a** (30 mg, 0.02 mmol) and a 30-fold excess of acetylacetone in a 1:1 mixture of CD<sub>2</sub>Cl<sub>2</sub>/CD<sub>3</sub>OD (2 mL) under nitrogen. The tube was pressurized with hydrogen to 50 bar at room temperature and then placed into a NMR probe

(16) (a) Mashima, K.; Kusano, K.; Ohta, T.; Noyori, R.; Takaya, H. *J. Chem. Soc., Chem. Commun.* **1989**, 1208. (b) Kitamura, M.; Ohkuma, T.; Inoue, S.; Sayo, N.; Kumobayashi, H.; Akutagawa, S.; Ohta, T.; Takaya, H.; Noyori, R. *J. Am. Chem. Soc.* **1988**, *110*, 629.

(17) MacNeil, P. A.; Roberts, N. K.; Bosnich, B. *J. Am. Chem. Soc.* **1981**, *103*, 2273.

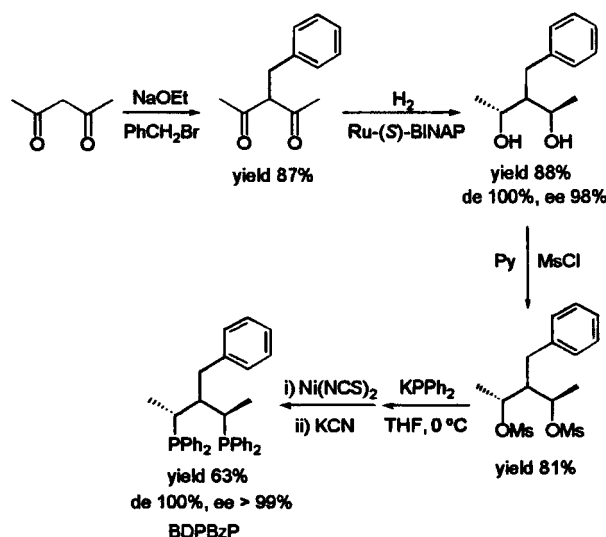
(18) Fryzuk, M. D.; Bosnich, B. *J. Am. Chem. Soc.* **1977**, *99*, 6262.

at 20 °C. The reaction was followed by variable-temperature  $^{31}\text{P}\{^1\text{H}\}$  and  $^1\text{H}$  NMR spectroscopy in the temperature range from 20 to 50 °C for an overall time of ca. 4 h. After 3 h at 50 °C, more than 90% of **6a** converted to a new product featured by two unresolved  $^{31}\text{P}\{^1\text{H}\}$  resonances centered at 31.2 and 71.5 ppm.  $^1\text{H}$  NMR spectroscopy showed the conversion (45%, 50 °C, 3 h) of acetylacetone, mainly to (*R*)-(*R*)-2,4-pentandiol, and the formation of catalytic amounts of HD. No resonance in the hydride region was observed. After the catalytic reaction was quenched by cooling to room temperature and depressurizing, the mixture was analyzed by GC, confirming the reduction of the diketone to the diol together with minor amounts of the monohydrogenated alcohol 4-hydroxypentan-2-one and of acetalization products (vide infra). A blank experiment carried out in the absence of acetylacetone gave a quite similar result except for the formation of the reduction products of acetylacetone (50% conversion of **6a** to the new product in 1 h at 50 °C). Under comparable experimental conditions but in neat  $\text{CD}_2\text{Cl}_2$ , **6a** was stable and acetylacetone was not hydrogenated.

**Synthesis of [(BDPBzP)( $\eta^2\text{-H}_2$ )ClRu( $\mu\text{-H}$ ) $_2$ RuCl( $\eta^2\text{-H}_2$ )(BDPBzP)] (**8**).** A suspension of **6a** (60 mg, 0.04 mmol) in methanol (20 mL) was transferred via a Teflon capillary into a 100 mL autoclave under argon. Argon was then replaced by hydrogen with three cycles 5 bar/1 bar. The autoclave was finally charged with 50 bar of  $\text{H}_2$  and stirred at 50 °C for 3 days. After this time, the reactor was cooled to room temperature and a 0.5 mL sample of the reaction mixture was transferred under  $\text{H}_2$  via a Teflon capillary into an NMR Evan's tube (whose inner tube was charged with  $\text{MeOH-}d_4$  in order to provide a lock signal).  $^{31}\text{P}\{^1\text{H}\}$ ,  $^1\text{H}$ ,  $^1\text{H}\{^{31}\text{P}\}$ , and  $^1\text{H}\{^{31}\text{P}\}_{\text{selective}}$  NMR experiments showed the quantitative formation of a product which is assigned the nonclassical dimeric structure [(BDPBzP)( $\eta^2\text{-H}_2$ )ClRu( $\mu\text{-H}$ ) $_2$ RuCl( $\eta^2\text{-H}_2$ )(BDPBzP)].  $^1\text{H}$  NMR ( $\text{CH}_3\text{OH}$ , 294 K, 500.13 MHz): 1.14 (dd, 6H,  $\text{CH}_3\text{-CP}_2$ ), 1.02 (dd, 6H,  $\text{CH}_3\text{CP}_1$ ),  $-9.56$  (AA' [ $^1\text{H}$ ]  $\text{M}_2\text{XX}'$  [ $^{31}\text{P}$ ] spin system, 2H, ( $\mu\text{-H}$ ) $_2$ ,  $^2J_{\text{HH}'}$  = 45.5,  $^2J_{\text{HP}_2}$  =  $^2J_{\text{HP}_2'}$  = 45.7,  $^2J_{\text{HP}_2}$  =  $^2J_{\text{HP}_2'}$  = 36.8,  $^2J_{\text{HP}_1}$  =  $^2J_{\text{HP}_1'}$  =  $^2J_{\text{HP}_1}$  =  $^2J_{\text{HP}_1'}$  = 9.3 Hz),  $-13.84$  (bs, 4H,  $\text{H}_2$ ).

**X-ray Crystal Structure Determination of 5.** Crystals of **5** were obtained by crystallization of the crude reaction product from  $\text{CH}_2\text{Cl}_2/i\text{-PrOH}$  under nitrogen. X-ray data were collected at room temperature on an Enraf-Nonius CAD4 diffractometer equipped with a graphite-oriented monochromator utilizing Mo K $\alpha$  radiation ( $\lambda$  = 0.71069 Å). The final unit cell parameters were obtained by least-squares refinement of the setting angles of 25 reflections that had been accurately centered on the diffractometer. The intensities of three standard reflections were measured every 120 min of X-ray exposure. No decay was observed. An empirical correction for the absorption effect was applied via  $\Psi$ -scan. The structure was solved by direct methods using the SIR92 program, and all of the non-hydrogen atoms were found through a series of  $F_o$  Fourier maps. Hydrogen atoms were introduced at calculated positions. The refinement was done by full-matrix least-squares calculations, initially with isotropic thermal parameters. The refinement, for 201 parameters and 4683 reflections with  $I > 2\sigma(I)$ , converged to  $R$  = 0.0604 ( $R_w$  = 0.1654 for all data). The absolute configuration was confirmed by the refinement of the Flack parameter. Models reached convergence with  $R = \sum(|F_o| - |F_c|)/\sum(F_o)$  and  $R_w = [\sum w(F_o - F_c)^2/\sum wF_o^4]^{1/2}$ . The calculations were carried out by using the SHELXL93<sup>19</sup> and ZORTEP programs.<sup>20</sup> Details of data collection and refinement are given in Table 1. The absolute configuration of each stereocenter was confirmed by the refinement of the Flack parameter ( $-0.06(6)$ ). Although the refinement of the

Scheme 1

Table 1. Crystal Data and Structure Refinement for **5**

empirical formula	$\text{C}_{48}\text{H}_{54}\text{Cl}_4\text{I}_2\text{P}_2\text{Ru}$
fw	1186.50
temperature, K	293(2)
wavelength, Å	0.71069
cryst syst	orthorhombic
space group	$P2_12_12_1$
unit cell dimens	$a = 15.534(5)$ Å, $\alpha = 90.000(5)^\circ$ $b = 21.490(5)$ Å, $\beta = 90.000(5)^\circ$ $c = 14.419(5)$ Å, $\gamma = 90.000(5)^\circ$
volume, Å <sup>3</sup>	4813(3)
Z	4
density (calcd), g/cm <sup>3</sup>	1.637
abs coeff, mm <sup>-1</sup>	1.929
$F(000)$	2348
crystal size, mm	$0.325 \times 0.3200 \times 0.325$
$\theta$ range for data collection	$1.62\text{--}24.97^\circ$
index ranges	$18 \geq h \geq 0$ , $25 \geq k \geq 0$ , $17 \geq l \geq 0$
no. of reflns collected	4683
no. of ind reflns	4683 [ $R(\text{int}) = 0.0000$ ]
refinement method	full-matrix least-squares on $F^2$
data/restraints/params	4683/1/201
goodness-of-fit on $F^2$	1.103
final $R$ indices [ $I > 2\sigma(I)$ ]	$R = 0.0604$ , $R_w = 0.1490$
$R$ indices (all data)	$R = 0.0888$ , $R_w = 0.1654$
absolute struct param	$-0.06(6)$
min corr factor	0.8744
max corr factor	0.9982
largest diff peak and hole, e/Å <sup>-3</sup>	1.688 and $-1.193$

structure converged, rather high values of residual electron density were observed, which is attributed to some disorder in the solvent region.

## Results and Discussion

**Synthesis and Characterization of the Chiral Ligand BDPBzP.** The novel chiral diphosphine ligand (*R*)-(*R*)-3-benzyl-2,4-bis(diphenylphosphino)pentane (BDPBzP) has been synthesized in good yield and excellent de and ee, through the reaction sequence shown in Scheme 1. The stereocenters in the C-2 and C-4 positions of the ligand backbone have been introduced by enantioselective hydrogenation of 3-benzyl-2,4-pentanedione (**1**) using [(*S*)-BINAP]Ru(*p*-cymene)Cl]Cl as chiral catalyst.<sup>16</sup> No loss of optical activity was observed upon nucleophilic attack by potassium diphenylphosphide at the stereocenters of the bis(mesylate) derivative

(19) Sheldrick, G. M. *SHELXL93*, Program for crystal structure refinement; University of Göttingen, 1993.

(20) Johnson, C. K. *ORTEP*, Per. ORNL-5138; Oak Ridge National Laboratory, Oak Ridge, TN, 1976, as modified by Zsolnai and Prizkow, Heidelberg University, 1994.

**Table 2.**  $^1\text{H}$  NMR Chemical Shifts (ppm) and Coupling Constants (Hz) for (*R*)-(*R*)-BDPBzP<sup>a</sup>

proton	$\delta$	$J$	proton	$\delta$
P <sub>1</sub> CH	3.43 (qndd)	$^3J_{\text{HCH}_3}$ 7.0, $^3J_{\text{HH}}$ 1.6, $^2J_{\text{HP}_1}$ 7.0, $^4J_{\text{HP}_2}$ 4.7	P <sub>1</sub> Ph'	<i>o</i> 7.68 (td)
P <sub>2</sub> CH	2.46 (qnt)	$^3J_{\text{HCH}_3}$ 7.4, $^3J_{\text{HH}}$ 2.7, $^2J_{\text{HP}_2}$ 7.4, $^4J_{\text{HP}_1}$ 2.7	<i>m</i>	7.39 <sup>b</sup>
P <sub>1</sub> C-CH <sub>3</sub>	1.23 (dd)	$^3J_{\text{HH}}$ 7.0, $^3J_{\text{HP}_1}$ 16.2	<i>p</i>	7.35 <sup>b</sup>
P <sub>2</sub> C-CH <sub>3</sub>	0.99 (dd)	$^3J_{\text{HH}}$ 7.4, $^3J_{\text{HP}_2}$ 13.5	P <sub>1</sub> Ph''	<i>o</i> 7.45 (td)
CH	2.03	$^3J_{\text{HH}}$ 1.6, $^3J_{\text{HH}}$ 2.7, $^3J_{\text{H}_\alpha\text{H}}$ 2.9, $^3J_{\text{H}_\beta\text{H}}$ 12.0	<i>m</i>	6.96 <sup>b</sup>
		$^3J_{\text{HP}_1}$ 11.3, $^3J_{\text{HP}_2}$ 7.4	<i>p</i>	7.14 (tq)
CH <sub>α</sub>	3.25 (dq)	$^2J_{\text{H}_\alpha\text{H}_\beta}$ 13.3, $^3J_{\text{H}_\alpha\text{H}}$ 2.9, $^4J_{\text{H}_\alpha\text{P}_1}$ 2.9, $^4J_{\text{H}_\alpha\text{P}_2}$	P <sub>2</sub> Ph'	<i>o</i> 7.23 <sup>b</sup>
CH <sub>β</sub>	2.75 (dd)	$^2J_{\text{H}_\alpha\text{H}_\beta}$ 13.3, $^3J_{\text{H}_\beta\text{H}}$ 12.0	<i>m</i>	7.21 <sup>b</sup>
Ph	<i>o</i> 7.04		<i>p</i>	7.20 <sup>b</sup>
	<i>m</i> 7.32 <sup>b</sup>		P <sub>2</sub> Ph''	<i>o</i> 6.69 (td)
	<i>p</i> 7.27 <sup>b</sup>		<i>m</i>	6.97 <sup>b</sup>
			<i>p</i>	7.00 (tq)

<sup>a</sup> 500.132 MHz, 294 K, CDCl<sub>3</sub>. Abbreviations: s, singlet; d, doublet; t, triplet; q, quartet; qn, quintet. Multiplet unless otherwise specified.<sup>b</sup> Partially overlapped with other resonances.**Table 3.**  $^{13}\text{C}$  NMR Chemical Shifts (ppm) and Coupling Constants (Hz) for (*R*)-(*R*)-BDPBzP<sup>a</sup>

carbon	$\delta$	$J$	carbon	$\delta$	$J$
P <sub>1</sub> C	30.58 (t)	$^1J_{\text{CP}}$ 11.1	P <sub>1</sub> Ph'	<i>i</i> 138.26 (d)	$^1J_{\text{CP}}$ 14.6
P <sub>2</sub> C	31.42 (t)	$^1J_{\text{CP}}$ 8.7	<i>o</i>	134.14 (d)	$^2J_{\text{CP}}$ 20.3
P <sub>1</sub> C-CH <sub>3</sub>	13.81 (d)	$^2J_{\text{CP}}$ 19.0	<i>m</i>	128.29 (d)	$^3J_{\text{CP}}$ 7.4
P <sub>2</sub> C-CH <sub>3</sub>	12.48 (d)	$^2J_{\text{CP}}$ 16.4	<i>p</i>	128.83 (s)	
CH	40.11 (t)	$^2J_{\text{CP}}$ 15.1	P <sub>1</sub> Ph''	<i>i</i> 136.26 (d)	$^1J_{\text{CP}}$ 13.5
CH <sub>2</sub>	33.85 (t)	$^3J_{\text{CP}}$ 8.3	<i>o</i>	133.98 (d)	$^2J_{\text{CP}}$ 19.6
Ph	<i>i</i> 141.05 (s)		<i>m</i>	128.00 <sup>b</sup>	
	<i>o</i> 129.64 (s)		<i>p</i>	127.96 (s)	
	<i>m</i> 128.15 (s)		P <sub>2</sub> Ph'	<i>i</i> 137.13 (d)	$^1J_{\text{CP}}$ 14.0
	<i>p</i> 125.94 (s)		<i>o</i>	134.06 (d)	$^2J_{\text{CP}}$ 20.5
			<i>m</i>	128.62 (d)	$^3J_{\text{CP}}$ 12.3
			<i>p</i>	128.06 (s)	
			P <sub>2</sub> Ph''	<i>i</i> 136.16 (d)	$^1J_{\text{CP}}$ 11.8
			<i>o</i>	132.81 (d)	$^2J_{\text{CP}}$ 18.8
			<i>m</i>	128.00 <sup>b</sup>	
			<i>p</i>	128.67 (s)	

<sup>a</sup> 125.76 MHz, 294 K, CDCl<sub>3</sub>. Abbreviations: s, singlet; d, doublet; t, triplet. <sup>b</sup> Partially overlapped with other resonances.**Table 4.**  $^{31}\text{P}\{^1\text{H}\}$  NMR Data for L = (*R*)-(*R*)-BDPBzP Complexes<sup>a</sup>

compound	$\delta$ P <sub>1</sub>	$\delta$ P <sub>2</sub>	$J$
L <sup>b</sup> ( <b>4</b> )	-1.24	-10.73	$J_{\text{PP}}$ 0.0
[LRu( <i>p</i> -cymene)I]I ( <b>5</b> )	45.36	33.43	$^2J_{\text{PP}}$ 57.2
L <sub>2</sub> Ru <sub>2</sub> (μ-Cl) <sub>3</sub> (DMSO)Cl <sup>c</sup> ( <b>6a</b> )	73.32 (A), 59.21 (B)	56.29 (A), 33.74 (B)	$^2J_{\text{PP(A)}}$ 51.7, $^2J_{\text{PP(B)}}$ 41.0
L <sub>2</sub> Ru <sub>2</sub> (μ-Cl) <sub>3</sub> (DMSO)Cl <sup>c</sup> ( <b>6b</b> )	69.97 (A), 60.88 (B)	58.34 (A), 40.54 (B)	$^2J_{\text{PP(A)}}$ 50.3, $^2J_{\text{PP(B)}}$ 42.0
[LRuCl(CH <sub>3</sub> CN) <sub>3</sub> ]OTf <sup>f</sup> ( <b>7</b> )	59.97	44.82	$^2J_{\text{PP}}$ 47.7
L <sub>2</sub> Ru <sub>2</sub> (μ-H) <sub>2</sub> (η <sup>2</sup> -H <sub>2</sub> ) <sub>2</sub> Cl <sub>2</sub> <sup>e,b</sup> ( <b>8</b> )	71.08	31.09	AA'XX' spin system
L <sub>2</sub> Ru <sub>2</sub> (μ-Cl) <sub>2</sub> (DMSO) <sub>2</sub> Cl <sup>d</sup> ( <b>9</b> )	54.39	48.57	$^2J_{\text{PP}}$ 41.1

<sup>a</sup> Chemical shifts in ppm, coupling constants in Hz, 81.01 MHz, 294 K, CDCl<sub>3</sub>. <sup>b</sup> 202.46 MHz. <sup>c</sup> C<sub>6</sub>D<sub>6</sub>. <sup>d</sup> DMSO-*d*<sub>6</sub>. <sup>e</sup> CH<sub>3</sub>OH. <sup>f</sup> CD<sub>2</sub>Cl<sub>2</sub>.

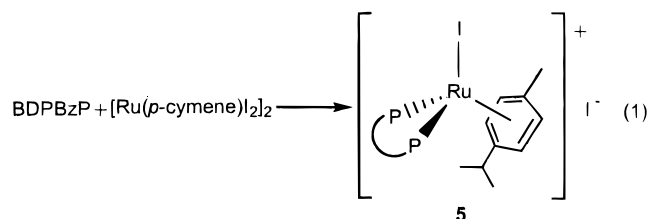
**3.** The purification of the diphosphine ligand was achieved by isolation of its Ni(II) thiocyanate complex, followed by cyanolysis with KCN.<sup>17,18</sup> Similar procedures have already been used for the synthesis of other chiral diphosphine ligands, including optically pure 2,4-bis-(diphenylphosphino)pentane (BDPP).<sup>1d,17,21</sup>

The ligand BDPBzP has been characterized by NMR spectroscopy. The relative  $^1\text{H}$ ,  $^{13}\text{C}\{^1\text{H}\}$ , and  $^{31}\text{P}\{^1\text{H}\}$  NMR data are reported in Tables 2, 3, and 4, respectively. The two CH(Me)PPh<sub>2</sub> moieties of BDPBzP are diastereotopic, as shown by two  $^{31}\text{P}\{^1\text{H}\}$  NMR signals at -1.24 (P<sub>1</sub>) and -10.73 ppm (P<sub>2</sub>) and by two distinct sets of  $^1\text{H}$  and  $^{13}\text{C}\{^1\text{H}\}$  NMR signals for the methyl, methine, and methylene groups.

**Synthesis and Characterization of Ruthenium Complexes with the BDPBzP Ligand.** Starting from appropriate organometallic precursors (eqs 1–3), the ligand BDPBzP has been employed to prepare the *p*-cymene complex [(BDPBzP)Ru(*p*-cymene)I]I·2CH<sub>2</sub>Cl<sub>2</sub>

(**5**), the μ-Cl<sub>3</sub> dimer [(BDPBzP)(DMSO)Ru(μ-Cl)<sub>3</sub>RuCl-(BDPBzP)] (**6a**), and the acetonitrile complex [(BDPBzP)RuCl(CH<sub>3</sub>CN)<sub>3</sub>]OTf (**7**). All the new complexes have been characterized in solution by multinuclear NMR spectroscopy.  $^{31}\text{P}\{^1\text{H}\}$  NMR data are shown in Table 4, while selected  $^1\text{H}$  and  $^{13}\text{C}\{^1\text{H}\}$  NMR data are reported in the Experimental Section.

**Complex 5.** Reaction of BDPBzP with [Ru(*p*-cymene)-I<sub>2</sub>]<sub>2</sub> in CH<sub>2</sub>Cl<sub>2</sub>/methanol gave crystals of the stable complex **5** (eq 1). The  $^1\text{H}$  NMR spectrum (CDCl<sub>3</sub>, 294

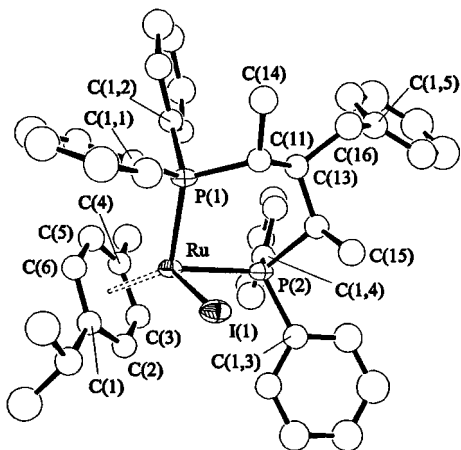




**Table 5. Selected Bond Lengths (Å) and Angles (deg) for **5****

Ru–C(1)	2.35(1)	C(1)–C(2)	1.43(2)
Ru–C(2)	2.27(1)	C(2)–C(3)	1.38(2)
Ru–C(3)	2.26(1)	C(3)–C(4)	1.43(2)
Ru–C(4)	2.31(1)	C(4)–C(5)	1.39(2)
Ru–C(5)	2.22(1)	C(5)–C(6)	1.44(2)
Ru–C(6)	2.29(1)	C(1)–C(6)	1.38(2)
Ru–P(1)	2.340(3)	P(1)–Ru–I(1)	87.44(9)
Ru–P(2)	2.340(4)	P(2)–Ru–I(1)	85.92(9)
Ru–I(1)	2.706(1)	P(1)–Ru–P(2)	91.53(13)
C <sub>6</sub> H <sub>4</sub> –Ru(1)	1.798	C <sub>6</sub> H <sub>4</sub> –Ru–I(1) <sup>a</sup>	122.66
		C <sub>6</sub> H <sub>4</sub> –Ru–P(1)	124.98
		C <sub>6</sub> H <sub>4</sub> –Ru–P(2)	131.12

<sup>a</sup> C<sub>6</sub>H<sub>4</sub> indicates the centroid of the benzenoid ring coordinated to ruthenium.

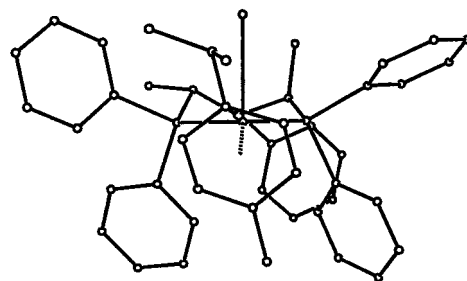
**Figure 1.** ORTEP drawing of the complex cation in [(BDBPBzP)Ru(*p*-cymene)I]I·2CH<sub>2</sub>Cl<sub>2</sub> (**5**). The 30% thermal ellipsoids for the carbon atoms are not shown for simplicity.

(s, 2H), 5.62 (dd, 1H), 4.96 (d, 1H).<sup>22</sup> The methyl group of the coordinated *p*-cymene appears as a singlet at 0.92 ppm, while the two diastereotopic CH(CH<sub>3</sub>)<sub>2</sub> groups give doublets at 1.22 and 0.70 ppm.

Similar *p*-cymene complexes containing the chiral diphosphine ligands BINAP and BICHEP have previously been synthesized and employed in asymmetric hydrogenation of ketones.<sup>16a,23</sup>

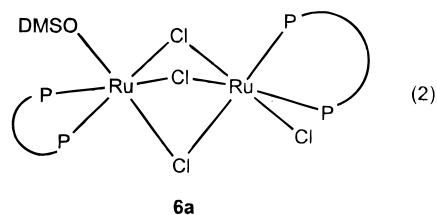
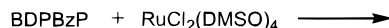
A single-crystal X-ray diffraction analysis has been carried out on **5**. Selected bond distances and angles are reported in Table 5, and an ORTEP view of the complex cation is shown in Figure 1.

The *p*-cymene molecule in **5** displays an η<sup>6</sup>-coordination mode with nearly equivalent C–Ru distances (2.22–2.35 Å) and alternated C–C distances (1.43 and 1.38 Å), the benzenoid ring being substantially planar (distances of the carbon atoms from the least-squares plane 0.04–0.03 Å). The coordination geometry around the metal center can be described as either a distorted octahedron or a distorted tetrahedron according to whether the coordinated arene is treated as occupying either one or three coordination sites. In the tetrahedral picture, the distortion from the idealized geometry is mainly due to the displacement of the ruthenium atom from the I(1)–P(1)–P(2) face so as to decrease the P(1)–Ru(1)–I(1), P(2)–Ru(1)–I(1), and P(1)–Ru(1)–P(2) angles

**Figure 2.** Ball and stick view of the complex cation [(BDBPBzP)Ru(*p*-cymene)I]<sup>+</sup> in the edge plane P(1)–Ru–P(2).

[87.44(9)°, 85.92(9)°, and 91.53(13)°, respectively] and increase the C<sub>6</sub>H<sub>4</sub>–Ru(1)–I(1), C<sub>6</sub>H<sub>4</sub>–Ru(1)–P(1), and C<sub>6</sub>H<sub>4</sub>–Ru(1)–P(2) angles [122.66°, 124.98°, and 131.12°, respectively].<sup>24</sup> Irrespective of the geometry, the six-membered chelate ring assumes a distorted chair conformation in which an iodide, the methyl group at the C(15) carbon stereocenter, and two phenylphosphino rings (C(1,4) and C(1,2)) are pseudoaxial, while the C(14) methyl and benzyl groups, the *p*-cymene ligand, and the other two phenylphosphino rings (C(1,1) and C(1,3)) are pseudoequatorial. A ball-and-stick view of this arrangement is provided in Figure 2. The benzyl group is twisted so that the phenyl ring lies in the same portion of space as the two pseudoaxial phenylphosphine rings [C(11)–C(13)–C(16)–C(1,5) = –167.7°]. The *p*-cymene ligand has a “longitudinal” arrangement with respect to the six-membered chelate ring [C(4)–C<sub>6</sub>H<sub>4</sub>–Ru–P(1) = 78.4°]. Interestingly, the two Ru–P bond lengths are identical [2.340 Å].

**Complex 6a.** The reaction of RuCl<sub>2</sub>(DMSO)<sub>4</sub> with BDBPBzP in refluxing ethanol gives the μ-Cl<sub>3</sub> dimer **6a** as yellow-orange microcrystals (eq 2).



Compound **6a** is soluble at room temperature in CH<sub>2</sub>Cl<sub>2</sub>, C<sub>6</sub>H<sub>6</sub>, and THF, in which it behaves as a nonelectrolyte. The IR band observed at 1110 cm<sup>−1</sup> is consistent with the presence of an η<sup>1</sup>-S sulfoxide ligand.<sup>25,26</sup> The DMSO ligand seems to be important for the stabilization of the complex, as shown by the fact that the substitution of RuCl<sub>2</sub>(PPh<sub>3</sub>)<sub>3</sub> for RuCl<sub>2</sub>(DMSO)<sub>4</sub> as starting Ru material did not lead to the formation of any stable product. The unsymmetrical arrangement of the diphosphine ligands in **6a**, as shown in Scheme 2, has been assigned on the basis of an in-depth NMR study. Analogous transoid structures have previously been

(22) Bennet, M. A. In *Comprehensive Organometallic Chemistry*; Wilkinson, G., Stone, F. G. A., Abel, E. W., Eds.; Pergamon Press: Oxford, 1995; Vol. 7, Chapter 9.

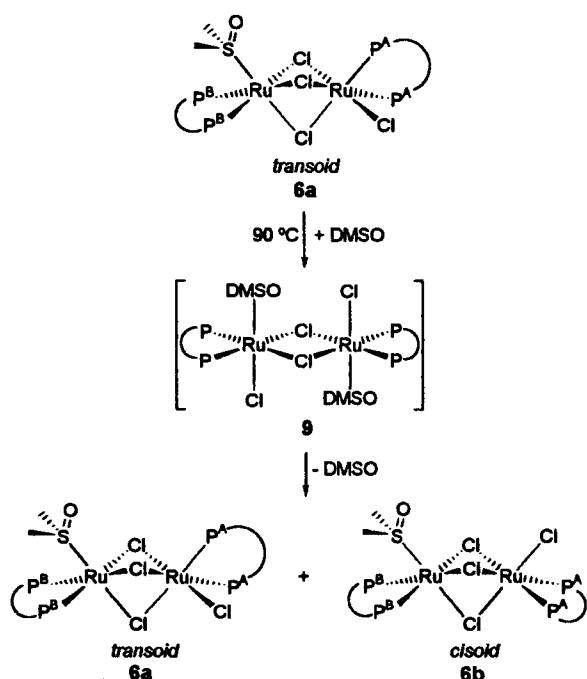
(23) Miyashita, A.; Chiba, T.; Nohira, H.; Takaya, H. *Abstract of 38th Symposium on Organometallic Chemistry*; Kyoto, 1991, B216.

(24) Distances of Ru from the least-squares planes: Ru–[I(1)–P(1)–P(2)] = 1.45 Å, Ru–[P(1)–P(2)–C<sub>6</sub>H<sub>4</sub>] = 0.41 Å, Ru–[I(1)–P(1)–C<sub>6</sub>H<sub>4</sub>] = –0.61 Å, Ru–[I(1)–P(2)–C<sub>6</sub>H<sub>4</sub>] = 0.54 Å.

(25) Joshi, A. M.; Thorburn, I. S.; Rettig, S. J.; James, B. R. *Inorg. Chim. Acta* **1992**, 198–200, 283.

(26) (a) Jaswal, J. S.; Rettig, S. J.; James, B. R. *Can. J. Chem.* **1990**, 68, 1808. (b) Evans, I. P.; Spencer, A.; Wilkinson, G. *J. Chem. Soc., Dalton Trans.* **1973**, 204.

Scheme 2



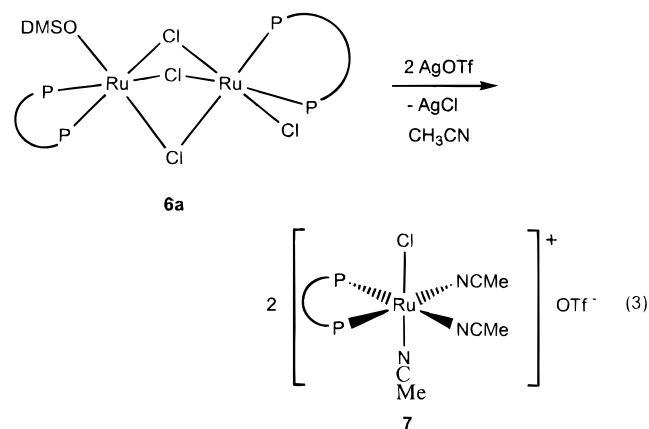
reported for the related complexes  $[(\text{DMSO})(\text{dppb})\text{-Ru}(\mu\text{-Cl})_3\text{RuCl}(\text{dppb})]$ ,<sup>25</sup>  $[(\eta^2\text{-H}_2)(\text{dppb})\text{Ru}(\mu\text{-Cl})_3\text{RuCl}(\text{dppb})]$ ,<sup>27</sup> and  $[(\text{CS})(\text{PPh}_3)_2\text{Ru}(\mu\text{-Cl})_3\text{RuCl}(\text{PPh}_3)_2]$ ,<sup>28</sup> where dbbp is the achiral ligand 1,4-bis-(diphenylphosphino)-butane.

The  $^{31}\text{P}\{^1\text{H}\}$ ,  $^1\text{H}$ , and  $^{13}\text{C}\{^1\text{H}\}$  NMR spectra of **6a** contain two independent sets of signals for each diphosphine ligand, denoted as  $\text{P}_1^{\text{A}}\text{-P}_2^{\text{A}}$  and  $\text{P}_1^{\text{B}}\text{-P}_2^{\text{B}}$ , with  $\delta \text{P}_1^{\text{A}}$  73.32,  $\delta \text{P}_1^{\text{B}}$  59.21,  $\delta \text{P}_2^{\text{A}}$  56.29,  $\delta \text{P}_2^{\text{B}}$  33.74 ppm ( $^2J_{\text{PP}(\text{A})}$ , 51.7;  $^2J_{\text{PP}(\text{B})}$ , 41.0 Hz, in  $\text{C}_6\text{D}_6$ ). The methyl groups of the coordinated DMSO molecule appear as two diastereotopic singlets at  $\delta$  2.94 and 2.75 ppm in the  $^1\text{H}$  NMR spectrum, while they are incidentally isochronous in the  $^{13}\text{C}$  NMR spectrum (singlet at  $\delta$  52.21 ppm). On the basis of a cis-influence criterion,<sup>29,25</sup> the diphosphine ligand  $\text{P}^{\text{B}}\text{-P}^{\text{B}}$  with phosphorus resonances at higher field as compared to those of  $\text{P}^{\text{A}}\text{-P}^{\text{A}}$  may be assigned as the one bonded to the Ru atom coordinated by the DMSO molecule. This assignment was unequivocally confirmed by the strong NOE interactions observed between the  $(\text{CH}_3)_2\text{SO}$  protons and the  $\text{CH}_3\text{CP}_2^{\text{B}}$  and  $o\text{-PhP}^{\text{B}}$  protons that were readily identified from a 2D  $^1\text{H}\text{-}^{31}\text{P}$  NMR correlation.

Besides the unsymmetrical transoid structure proposed for **6a**, a dimer such as  $[(\text{BDPBzP})_2\text{Ru}_2(\mu\text{-Cl})_3(\text{DMSO})\text{Cl}]$  may exist also in the cisoid form sketched in Scheme 2, featuring a symmetrical arrangement of the diphosphine ligands. However, no evidence for either cis/trans interconversion or formation of other products was observed by NMR spectroscopy on  $\text{C}_6\text{D}_6$ , THF- $d_6$ , or  $\text{CD}_2\text{Cl}_2$  solutions of **6a** in the temperature range from 294 to 340 K. Only by heating a solution of **6a** in DMSO-

$d_6$  under argon at 90 °C was a new compound slowly formed, which became the only product detectable by in situ NMR spectroscopy after 2 h. This new complex, featuring the magnetic equivalence of the diphosphine ligands (broad signals,  $\delta \text{P}_1$ , 54.39,  $\delta \text{P}_2$ , 48.57 ppm;  $^2J_{\text{PP}}$  41.1 Hz, DMSO- $d_6$ , 23 °C), is most likely the symmetric  $\mu\text{-Cl}_2$  dimer  $[(\text{P-P})\text{Cl}(\text{DMSO})\text{Ru}(\mu\text{-Cl})_2\text{Ru}(\text{DMSO})\text{Cl}(\text{P-P})]$  (**9**), which is structurally similar to  $[\text{RuCl}(\text{PPh}_3)_2\text{-}(\text{RCN})]_2(\mu\text{-Cl})_2$ <sup>30</sup> and  $[\text{RuCl}(\text{dppb})\text{py}]_2(\mu\text{-Cl})_2$ .<sup>27</sup> Unfortunately, **9** could be observed only by NMR spectroscopy in DMSO solution, and all our attempts to isolate it in the solid state were unsuccessful. However, when the solvent was removed from a solution of **9** under reduced pressure and the solid residue was dissolved in  $\text{C}_6\text{D}_6$  under argon, the  $^{31}\text{P}\{^1\text{H}\}$  NMR analysis showed the product to be a ca. 2:1 mixture of **6a** and of another product that is tentatively assigned the symmetric cisoid structure **6b** (Scheme 2). This structural assignment has been made on the basis of the simple symmetry criterion according to which the chemical shift difference  $\Delta\delta(\text{P}_1\text{-P}_2)$  for each diphosphine ligand in the dimer is expected to be larger for the asymmetric structure than for the symmetric one.<sup>28,31</sup> Although the cisoid structure of **6b** remains our favorite choice on the basis of the  $^{31}\text{P}$  chemical shifts, one cannot rule out that this isomer may differentiate from **6a** by a different orientation of the benzyl groups.

**Complex 7.** Treatment of **6a** with 2 equiv of silver triflate in acetonitrile solution yields monomeric Ru(II)-tris(acetonitrile) complex **7** (eq 3). A similar procedure has previously been employed to prepare the dppb congener  $[(\text{dppb})\text{RuCl}(\text{CH}_3\text{CN})_3]\text{PF}_6$ .<sup>32</sup>



The solid-state IR spectrum of **7** shows absorptions at 2328, 2314, and 2310  $\text{cm}^{-1}$ , characteristic of coordinated  $\text{CH}_3\text{CN}$  molecules.<sup>33,34</sup> Consistent with the presence of three nonequivalent acetonitrile ligands, three singlets at 2.16, 1.92, and 1.84 ppm are observed in the

(27) MacFarlane, K. S.; Thorburn, I. S.; Cyr, P. W.; Chau, D. E. K.-Y.; Rettig, S. J.; James, B. R. *Inorg. Chim. Acta* **1998**, 270, 130.

(28) Stephenson, T. A.; Switkes, E. S.; Armit, P. *J. Chem. Soc., Dalton Trans.* **1974**, 1134.

(29) (a) Pregosin, P. S.; Kunz, R. W.  $^{31}\text{P}$  and  $^{13}\text{C}$  NMR of Transition Metal Phosphine Complexes; Diehl, P., Fluck, E., Kosfeld, R., Eds.; Springer-Verlag: Berlin, 1979. (b) Appleton, T. G.; Clark, H. C.; Manzer, L. E. *Coord. Chem. Rev.* **1973**, 10, 335. (c) Meek, D. W.; Mazanec, T. J. *Acc. Chem. Res.* **1981**, 14, 266.

(30) Cole-Hamilton, D. J.; Wilkinson, G. *J. Chem. Soc., Dalton Trans.* **1979**, 1283.

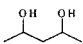
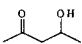
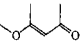
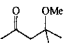
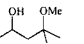
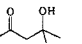
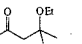
(31)  $\Delta\delta(\text{P}_1\text{-P}_2) = ^{31}\text{P}\{^1\text{H}\}$  NMR chemical shifts difference (ppm) shown by the phosphorus atoms of each diphosphine ligand.  $\Delta\delta(\text{P}_1^{\text{A}}\text{-P}_2^{\text{A}})$  **6b** = 11.7,  $\Delta\delta(\text{P}_1^{\text{A}}\text{-P}_2^{\text{A}})$  **6a** = 17.0 ppm.  $\Delta\delta(\text{P}_1^{\text{B}}\text{-P}_2^{\text{B}})$  **6b** = 20.4,  $\Delta\delta(\text{P}_1^{\text{B}}\text{-P}_2^{\text{B}})$  **6a** = 25.5 ppm.

(32) Thorburn, I. S.; Rettig, S. J.; James, B. R. *J. Organomet. Chem.* **1985**, 296, 103.

(33) Barbaro, P.; Bianchini, C.; Togni, A. *Organometallics* **1997**, 16, 3004.

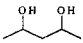
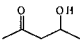
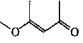
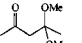
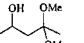
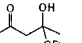
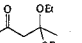
(34) (a) Nakamoto, K. *Infrared and Raman Spectra of Inorganic and Coordination Compounds*; Wiley: New York, 1986. (b) Sekine, M.; Harman, W. D.; Taube, H. *Inorg. Chem.* **1988**, 27, 3604. (c) Albinati, A.; Jiang, Q.; Rügger, H.; Venanzi, L. M. *Inorg. Chem.* **1993**, 32, 4940.

**Table 6. Asymmetric Hydrogenation of Acetylacetone Catalyzed by [(BDPBzP)RuCl(NCMe)<sub>3</sub>]OTf (7)<sup>a</sup>**

entry	solvent	S/Cat mol.ratio	T (°C)	time (h)	H <sub>2</sub> (atm)	 yield <sup>b</sup> , ee <sup>c</sup>	 yield <sup>b</sup> , ee (%)	 yield <sup>b</sup> (%)	 yield <sup>b</sup> (%)	 yield <sup>b</sup> (%)	 yield <sup>b</sup> (%)	 yield <sup>b</sup> (%)
1	MeOH	80	r.t.	48	50			17.5	50.2			
2	EtOH	80	r.t.	48	50		2.2				17.1	14.3
3	EtOH	80	40	48	50	6.2, 91.0	34.2, 69.8				14.7	4.7
4	EtOH	80	60	48	50	96.9, 82.9	0.6					

<sup>a</sup> BDPBzP = 3-Benzyl-2,4-bis(diphenylphosphino)pentane. Reaction conditions: Ru (0.01 mmol), solvent (20 mL). <sup>b</sup> GC, reaction mixture, average value of 3 runs. <sup>c</sup> (*R*)-(*R*)-enantiomer. No meso compound detected.

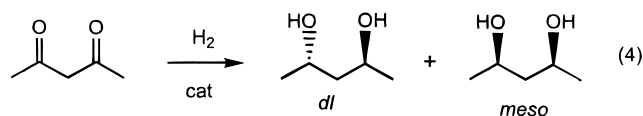
**Table 7. Asymmetric Hydrogenation of Acetylacetone Catalyzed by (BDPBzP)<sub>2</sub>Ru<sub>2</sub>(μ-Cl)<sub>3</sub>(DMSO)Cl (6a)<sup>a</sup>**

entry	solvent	S/Cat mol.ratio	T (°C)	time (h)	H <sub>2</sub> (atm)	 yield <sup>b</sup> , ee <sup>c</sup>	 yield <sup>b</sup> , ee (%)	 yield <sup>b</sup> (%)	 yield <sup>b</sup> (%)	 yield <sup>b</sup> (%)	 yield <sup>b</sup> (%)	 yield <sup>b</sup> (%)
1	MeOH	80	r.t.	48	70	18.2, 98.9	22.5, 55.0	14.7	26.2	6.6		
2	MeOH	80	40	24	50	93.5, 86.2	2.5					
3	EtOH	80	r.t.	48	50		12.1, 65.2				3.7	11.8
4	EtOH	80	40	24	50	95.1, 92.8	2.3, 14.2				1.4	
5	EtOH	80	60	24	50	99.4, 90.4	0.6					
6	EtOH	80	80	24	50	92.1, 91.7	4.0, 30.9					
7	EtOH	500	40	48	50	94.0, 91.2	2.6, 15.3				0.3	
8	EtOH	500	40	24	50	5.6, 98.6	38.9, 76.5				14.8	4.0
9	EtOH	500	r.t.	7	50	83.2, 95.2	4.9, 33.9				2.4	0.6

<sup>a</sup> BDPBzP = 3-Benzyl-2,4-bis(diphenylphosphino)pentane. Reaction conditions: Ru (0.01 mmol), solvent (20 mL). <sup>b</sup> GC, reaction mixture, average value of 3 runs. <sup>c</sup> (*R*)-(*R*)-enantiomer. No meso compound detected.

<sup>1</sup>H NMR spectrum (CD<sub>2</sub>Cl<sub>2</sub>, 294 K). Moreover, the separation of the <sup>31</sup>P NMR signals is comparable to that observed for the free diphosphine ligand, which indicates the presence of two identical ligands trans to the phosphorus atoms.<sup>29</sup>

**Enantioselective Hydrogenation of Acetylacetone to (*R*)-(*R*)-2,4-Pentanediol.** For a preliminary evaluation of the catalytic efficiency and enantioselectivity of metal complexes containing the BDPBzP ligand, we examined the hydrogenation of a representative substrate such as the β-diketone acetylacetone (eq 4). This



reaction generally affords mixtures of DL and *meso*-2,4-pentanediol. Enantioselectivities for the former product as high as 100% have been obtained by BINAP–Ru(II) catalysis.<sup>16</sup> Excellent results in terms of both diastereoselectivity and enantioselectivity have also been achieved using Ru(II) catalysts containing other C<sub>2</sub>-symmetric diphosphines such as BIPHEMP and DUPHOS-like 1,2-bis(phosphetano)benzenes.<sup>5,35</sup> No report has ever appeared describing the enantioselective hydrogenation of β-diketones by optically pure BDDP metal complexes.

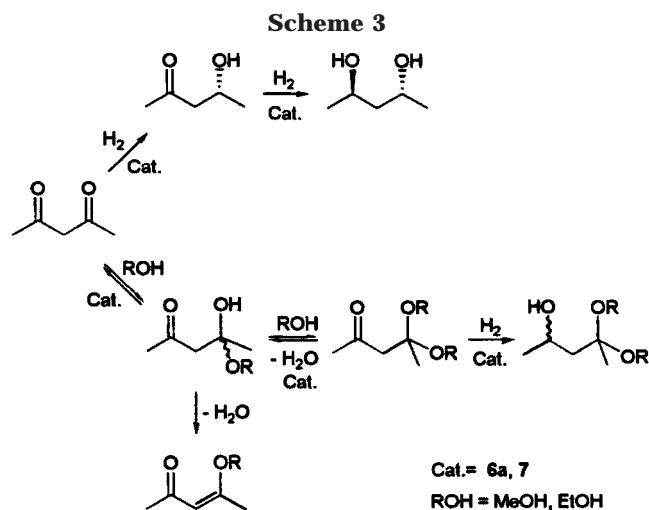
The hydrogenation reactions assisted by the BDPBzP Ru(II) complexes have been performed at a pressure of 50 bar H<sub>2</sub> in the temperature range from 20 to 80 °C with a maximum substrate/catalyst ratio of 500. Methanol and ethanol are suitable solvents for this reaction, which does not appreciably occur in C<sub>6</sub>H<sub>6</sub>, MeCN, THF, CH<sub>2</sub>Cl<sub>2</sub>, or *i*-PrOH. In these conditions, both **6a** and **7** behave as effective catalyst precursors for the reduction of acetylacetone, while the *p*-cymene complex **5** is almost inactive, and therefore, after a preliminary screening of its reactivity, it was not studied further.

Selected results are reported in Tables 6 and 7, while Scheme 3 illustrates the distribution of products that can be obtained in alcoholic solvent depending on the experimental conditions. In general, the reactions go to completion in 24 h at 40 °C for an initial H<sub>2</sub> pressure of 50 bar.

In MeOH, the acetalization of the mono-hydrogenated product 4-hydroxypentan-2-one competes with the second reduction step, especially when the mononuclear precursor **7** is employed (Table 6). This drawback was substantially minimized using EtOH. In this solvent, both catalyst precursors catalyze the reduction of acetyl-

(35) (a) Mezzetti, A.; Consiglio, G. *J. Chem. Soc., Chem. Commun.* **1991**, 1675. (b) Mezzetti, A.; Tschumper, A.; Consiglio, G. *J. Chem. Soc., Dalton Trans.* **1995**, 49. (c) Buriak, J. M.; Klein, J. C.; Herrington, D. G.; Osborn, J. A. *Chem. Eur. J.* **2000**, *6*, 139.





acetone with very high diastereoselectivity (actually, *meso*-2,4-pentanediol was not detected by GC in all runs) and high enantioselectivity (>90% for quantitative conversion of the substrate, entry 5 of Table 7). The acetalization reactions are reversible, as shown by the runs performed with a substrate-to-catalyst ratio of 500 (entries 7 and 8 of Table 7), in which the concentration of the acetal decreases substantially by doubling the reaction time.

With both catalysts the sense of induction is the same; that is, BDPBzP yields (*R*)-(*R*)-2,4-pentanediol, which is a common feature to all the other chiral catalysts scrutinized for this reaction.<sup>5,16,35a,b</sup>

Like BINAP–Ru(II) catalysts,<sup>5,16</sup> the monohydrogenated intermediate (*R*)-4-hydroxy-pentan-2-one was obtained in appreciable yields only at low temperature or low conversion (entries 1, 8 of Table 7). The relative yields and ee's of the mono- and dihydrogenated products are consistent with the effect of a double stereodifferentiation process.<sup>16,35a,b,36</sup>

**In Situ Study of the Hydrogenation Reactions Catalyzed by **6a**.** Dinuclear Ru(II) complexes of the general formula [(P–P)ClRu( $\mu$ -Cl)<sub>2</sub>RuCl(P–P)], where the diphosphine P–P is either chiral or achiral, are extensively being used in homogeneous catalysis.<sup>16,35</sup> In most instances, the reaction with H<sub>2</sub> leads to the formation of catalytically active mononuclear hydride species. At least in one case, however, the formation of a nonclassical  $\eta^2$ -H<sub>2</sub> dimer was unambiguously established by Joshi and James.<sup>37</sup> Indeed, the complex [(dppb)ClRu( $\mu$ -Cl)<sub>2</sub>RuCl(dppb)] was found to react with H<sub>2</sub> in apolar solvents to give equilibrium concentrations of the adduct [(dppb)( $\eta^2$ -H<sub>2</sub>)Ru( $\mu$ -Cl)<sub>3</sub>RuCl(dppb)], which was isolated and completely characterized [dppb = 1,4-bis(diphenylphosphino)butane].<sup>27,37</sup> No evidence supporting the thermodynamic or kinetic instability of the  $\eta^2$ -H<sub>2</sub> adduct in the course of catalytic hydrogenation reactions has been provided, however.

Given the similarity between **6a** and the trichloro-bridged complexes [L(dppb)Ru( $\mu$ -Cl)<sub>3</sub>RuCl(dppb)] described by James, we decided to study the hydrogenation of acetylacetone assisted by **6a** using HPNMR spectroscopy.

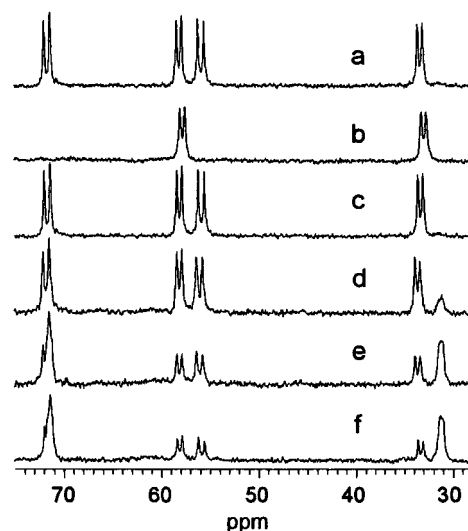
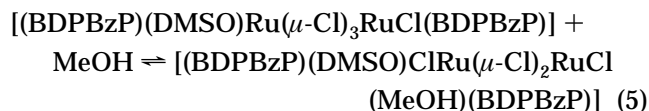


**Figure 3.**  $^{31}\text{P}\{^1\text{H}\}$  HPNMR spectra (sapphire tube, 81.01 MHz): [(BDPBzP)(DMSO)Ru( $\mu$ -Cl)<sub>3</sub>RuCl(BDPBzP)] (**6a**) and 20 equiv of acetylacetone. (a) CD<sub>2</sub>Cl<sub>2</sub>, Ar, 294 K. (b) MeOH-*d*<sub>4</sub>/CD<sub>2</sub>Cl<sub>2</sub> (1:1, v:v), Ar, 294 K. (c) 50 bar of H<sub>2</sub>, 294 K. (d) 50 bar of H<sub>2</sub>, 323 K, 15 min. (e) 50 bar of H<sub>2</sub>, 323 K, 1 h. (f) After depressurizing to 1 bar H<sub>2</sub>, 294 K.

copy. The catalyst precursor **6a** is not sufficiently soluble in MeOH to allow for an in situ study of the hydrogenation of acetylacetone by NMR spectroscopy. To this purpose 1:1 (v:v) mixtures of MeOH-*d*<sub>4</sub> and CD<sub>2</sub>Cl<sub>2</sub> have been employed. Compound **6a** was thus dissolved in neat CD<sub>2</sub>Cl<sub>2</sub> to test its purity and stability. After both properties were positively addressed by NMR spectroscopy, a 2 mL solution of 20 equiv of acetylacetone in degassed MeOH-*d*<sub>4</sub> was introduced into the 10 mm sapphire tube via syringe under argon. As a result, the signals of the diphosphine P<sup>A</sup>–P<sup>A</sup>, i.e., that belonging to the “RuCl(P–P)” moiety, became very broad, almost merging into the baseline, while the signals of the diphosphine bound to the other Ru atom remained unchanged. This phenomenon is shown in traces a and b of Figure 3, which illustrates the overall HPNMR experiment as followed by  $^{31}\text{P}\{^1\text{H}\}$  NMR spectroscopy.

A very similar dynamic process on the NMR time scale has previously been reported to occur for [py-(dppb)Ru( $\mu$ -Cl)<sub>3</sub>RuCl(dppb)] (py = pyridine) when pyridine is added to a solution of the dimeric complex in CHCl<sub>3</sub>.<sup>27</sup> A rapid equilibrium involving trichloro- and dichloro-bridged species has been proposed to account for the selective and extensive broadening of the resonance due to the diphosphine bound to the Ru–Cl<sub>terminal</sub> moiety. An analogous mechanism, shown in eq 5, may well account for the selective broadening of the P<sup>A</sup>–P<sup>A</sup> diphosphine ligand in **6a**.



Any role of acetylacetone in the observed spectral change was ruled out by performing a blank experiment in the absence of substrate.

The occurrence of a fast and selective coordination/decoordination of MeOH at a Ru center in **6a** was confirmed by a variable-temperature NMR experiment

(36) Masamune, S.; Choy, W.; Petersen, J. S.; Sita, L. R. *Angew. Chem., Int. Ed. Engl.* **1985**, 24, 1.

(37) Joshi, A. M.; James, B. R. *J. Chem. Soc., Chem. Commun.* **1989**, 1785.

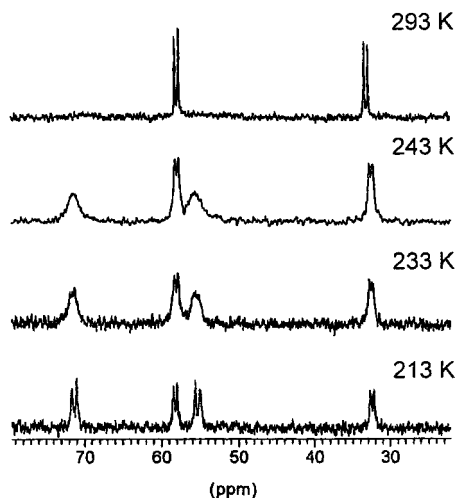


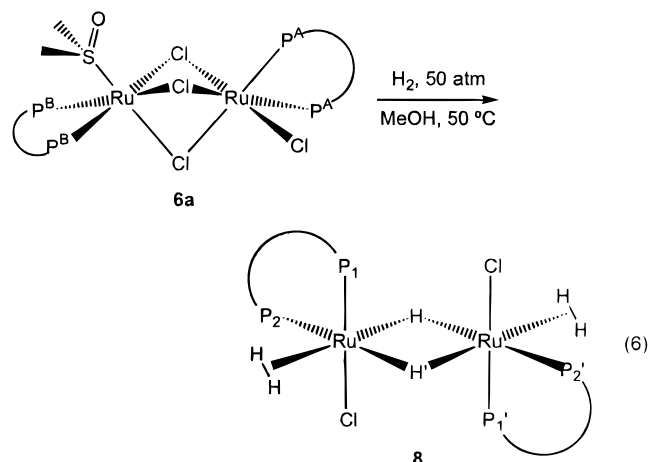
**Figure 4.** Variable-temperature  $^{31}\text{P}\{^1\text{H}\}$ NMR spectra (81.01 MHz) of **6a** in a 1:1 mixture of  $\text{CD}_2\text{Cl}_2/\text{CD}_3\text{OD}$  under argon.

independently performed in  $\text{CD}_2\text{Cl}_2/\text{MeOH}-d_4$ . Complex **6a** was dissolved in a 1:1 mixture of  $\text{CD}_2\text{Cl}_2/\text{CD}_3\text{OD}$  in a 5 mm NMR tube under argon. A  $^{31}\text{P}\{^1\text{H}\}$ NMR spectrum showed the reappearance of the signals due to  $\text{P}^{\text{A}}-\text{P}^{\text{A}}$  already at  $-30^\circ\text{C}$ . The dynamic process affecting **6a** was completely quenched at  $-60^\circ\text{C}$ . A series of variable-temperature NMR spectra are reported in Figure 4.

Interestingly, the fluxionality of **6a** in the presence of methanol was immediately quenched by replacing argon with 50 bar  $\text{H}_2$  (Figure 3, trace c). Except for a low-intensity featureless resonance at ca. 31 ppm, the resulting  $^{31}\text{P}$  NMR spectrum, however, was identical with that of the precursor under Ar in neat  $\text{CD}_2\text{Cl}_2$ . Nonetheless, the activation of  $\text{H}_2$  did occur as the formation of a catalytic amount of free HD (1:1:1 triplet at 4.4 ppm) was clearly evident in the  $^1\text{H}$  NMR spectrum. No hydrogenation of acetylacetone was observed. The interpretation of this series of events is not straightforward. The formation of HD implies that  $\text{H}_2$  is activated by a metal center (presumably the ruthenium atom in rapid coordination/decoordination of MeOH, see eq 5) and then undergoes H/D exchange by interaction with  $\text{MeOH}-d_4$ .<sup>37,38</sup> A model compound for this pathway is actually provided by the dimer  $[(\text{dppb})(\eta^2-\text{H}_2)\text{Ru}(\mu\text{-Cl})_3\text{RuCl}(\text{dppb})]$ .<sup>37</sup> This mechanistic picture obviously implies the involvement of a BDPBzP  $\eta^2-\text{H}_2$  derivative. As will be shown below, such a compound is indeed formed selectively and in high concentration at higher temperature. Traces of this product are also visible in the room-temperature spectrum ( $^{31}\text{P}$  resonance at 31 ppm in Figure 3, trace c), however. Just the interaction of  $\text{H}_2$  with **6a** to give an equilibrium concentration of this product may affect the equilibrium shown in eq 5 and ultimately quench the fluxionality observed in the absence of  $\text{H}_2$ .

When the temperature of the probe-head was increased to  $50^\circ\text{C}$  (Figure 3, trace d), a new product was actually formed, which can unequivocally be assigned the nonclassical polyhydride structure  $[(\text{BDPBzP})-$

$(\eta^2-\text{H}_2)\text{ClRu}(\mu\text{-H})_2\text{RuCl}(\eta^2-\text{H}_2)(\text{BDPBzP})]$  (**8**) on the basis of a detailed NMR analysis (eq 6).



The formation of **8** apparently implies the occurrence of two heterolytic splittings of  $\text{H}_2$  with production of HCl, a reaction path that is quite common for transition metal complexes in polar solvents.<sup>38</sup> No other species was observed by NMR spectroscopy even after the complete disappearance of **6a** and the total consumption of the substrate.

Compound **8** is featured by two  $^{31}\text{P}\{^1\text{H}\}$  resonances at 31.12 and 71.52 ppm, the latter falling just below the lower-field signal of the  $\text{P}^{\text{A}}-\text{P}^{\text{A}}$  ligand of complex **6a**. For this reason, it was not visible in trace c. The two resonances are unresolved due to deuterium incorporation (see below). With time, the concentration of **8** increased at the expense of that of **6a** (Figure 3, trace e, after 1 h at  $50^\circ\text{C}$ ). After the sample was heated for an overall time of 3 h, the probe-head was cooled to  $20^\circ\text{C}$ . A  $^{31}\text{P}$  NMR spectrum showed neither additional signals nor disappearance of the high-temperature ones. An identical spectrum was obtained after the tube was depressurized to 1 bar  $\text{H}_2$  (Figure 3, trace f), indicating that **8** is stable also at low  $\text{H}_2$  pressure. In contrast, when  $\text{H}_2$  was removed by sweeping the NMR tube with a flow of Ar or  $\text{N}_2$ , the compound decomposed to give several unidentified products.

Besides confirming the progressive consumption of the substrate to give (*R*)-(*R*)-2,4-pentanediol and (*R*)-4-hydroxypentan-2-one, a parallel  $^1\text{H}$  NMR study showed that **8** is featured by a triplet of triplets at  $-9.56$  ppm and by a complex multiplet at  $-13.84$  ppm, whose line shape clearly indicates the incorporation of deuterium with its characteristic 1:1:1 intensity pattern ( $J_{\text{HD}} = 28.0$  Hz). Also, the  $^1\text{H}$  NMR spectra showed that the formation of **8** was accompanied by that of free DMSO (singlet at 2.7 ppm).

The higher-field resonance in the hydride region disappeared completely on sweeping off the tube with a flow of argon. Consistently, all our attempts to isolate **8** in the solid state were unsuccessful due to its degradation to several unidentified products. Under comparable experimental conditions, the in situ hydrogenation of **6a** with 1 bar  $\text{H}_2$  did not produce **8**. However, once formed at high pressure, **8** showed a fairly good kinetic stability under 1 bar  $\text{H}_2$ . Accordingly,

(38) Jessop, P. G.; Morris, R. H. *Coord. Chem. Rev.* **1992**, *121*, 155.

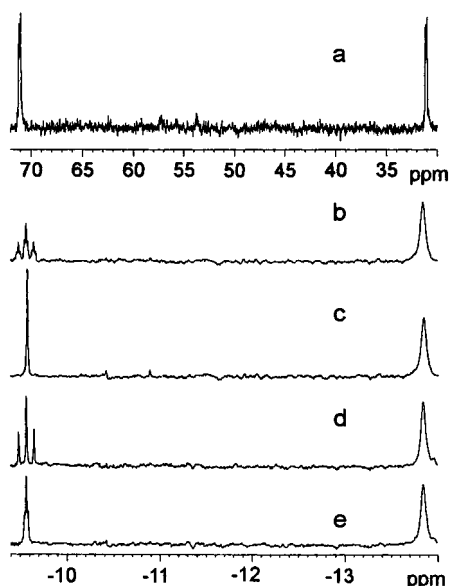


**Figure 5.** NMR spectra of  $[(\text{BDPBzP})(\eta^2\text{-H}_2)\text{ClRu}(\mu\text{-H})_2\text{RuCl}(\eta^2\text{-H}_2)(\text{BDPBzP})]$  (**8**) (MeOH, Evan's tube with MeOH- $d_4$ , 500.132 MHz, 294 K). (a)  $^{31}\text{P}\{^1\text{H}\}$  NMR spectrum. (b)  $^1\text{H}$  NMR spectrum in the hydride region. (c)  $^1\text{H}\{^{31}\text{P}\}$  NMR spectrum. (d)  $^1\text{H}\{^{31}\text{P}\}$  NMR spectrum selectively decoupled from the  $^{31}\text{P}$  signal at 71.08 ppm. (e)  $^1\text{H}\{^{31}\text{P}\}$  NMR spectrum selectively decoupled from the  $^{31}\text{P}$  signal 31.09 ppm.

a massive preparation of this compound was attempted by simply replacing the sapphire HPNMR tube with an autoclave.

Degassed methanol was introduced under argon into a 100 mL autoclave containing solid **6a**. The reactor was pressurized with 50 bar  $\text{H}_2$  and then heated to 50 °C with stirring. After 3 days at this temperature, the reactor was cooled to room temperature and a ca. 0.5 mL sample of the reaction mixture was transferred under a hydrogen atmosphere into an NMR Evan's tube whose inner tube was filled with  $\text{CD}_3\text{OD}$ . An in-depth NMR study (500.132 MHz, 294 K) showed that the complete and selective transformation of **6a** into **8** had occurred and allowed us to assign to the latter complex the dimeric structure shown in eq 6.

The  $^{31}\text{P}\{^1\text{H}\}$  NMR spectrum shows an AA'XX' spin system ( $A = \text{P}_1$ ,  $X = \text{P}_2$ ) and is thus consistent with the chemical equivalence of the two diphosphine ligands (Figure 5) (Table 4). The resonance observed at 71.08 ppm ( $\text{P}_1$ ) is assigned to the phosphorus atom trans to a chloride ligand on the basis of both its chemical shift and selective  $^1\text{H}\{^{31}\text{P}\}$  decoupling experiments. The values of the "bridging"  $^4J_{\text{PP}}$  coupling constants have been obtained from a computer simulation of the spectrum:  $^4J_{\text{P}_1\text{P}_2} = ^4J_{\text{P}_1\text{P}_2'} = 11.0$ ,  $^4J_{\text{P}_2\text{P}_2'} = 10.0$ ,  $^4J_{\text{P}_1\text{P}_1'} = 0.0$  Hz. The  $^1\text{H}$  NMR spectrum of **8** is consistent with the chemical equivalence of the two "Ru" subunits; for example, only one set of diastereotopic methyl  $\text{CH}_3\text{CP}_1$  and  $\text{CH}_3\text{CP}_2$  protons are observed at 1.02 and 1.14 ppm, respectively. The hydride region (Figure 5) contains a broad, unresolved singlet at -13.84, which is assigned to two symmetric  $\eta^2\text{-H}_2$  ligands on the basis of the  $T_1$  value of 16.8 ms (500.132 MHz, 294 K) as well as a  $J_{\text{HD}}$  value of 28.0 Hz in the deuterated isotopomer.<sup>37–40</sup> The two bridging hydride ligands give rise to a sharp AA'M<sub>2</sub>-XX' spin system ( $A = ^1\text{H}$ ,  $M = ^{31}\text{P}_1$ ,  $X = ^{31}\text{P}_2$ ) centered

at -9.56 ppm with  $^2J_{\text{HH}}$  and  $^2J_{\text{HP}}$  coupling constants obtained from a computer simulation (see Experimental Section). The  $\text{P}_1$  atoms can be assigned as those "out of the  $\text{Ru}_2(\mu\text{-H})_2$  plane" on the basis of  $^1\text{H}\{^{31}\text{P}\}$  selective-decoupling experiments ( $^2J_{\text{HP}} = 9.3$  Hz). The presence of two bridging hydrides and of two intact  $\text{H}_2$  ligands in the molecule was quantitatively determined by NMR integration comparing the relative intensity of the signals due to the  $\mu\text{-H}$ ,  $\eta^2\text{-H}_2$  groups and ligand  $\text{CH}_3$  groups.

Besides  $[(\text{dppb})(\eta^2\text{-H}_2)\text{Ru}(\mu\text{-Cl})_3\text{RuCl}(\text{dppb})]$  ( $T_1$  14 ms at 292 K,  $J_{\text{HD}}$  29.4 Hz),<sup>37</sup> other examples of nonclassical polyhydride bi-octahedral Ru(II) complexes have been reported:  $[(S\text{-biphemp})(\eta^2\text{-H}_2)\text{Ru}(\mu\text{-Cl})_3\text{RuCl}(S\text{-biphemp})]$  ( $T_{1\text{min}}$  8 ms at 233 K),<sup>40a</sup>  $[\text{Ru}_2(\text{H}_2)(\text{H})_4(\text{PCy}_3)_4]$  ( $T_1$  88 ms at 293 K, fluxional),<sup>40b</sup> and  $[(\text{P-N})(\eta^2\text{-H}_2)\text{Ru}(\mu\text{-H})(\mu\text{-Cl})_2\text{-Ru}(\text{P-N})]$  ( $T_1$  13.8 ms at 211 K) ( $\text{P-N} = \text{Fe}(\eta\text{-C}_5\text{H}_3\text{-CHMeNMe}_2)\text{P}(i\text{-Pr})_2(1,2)(\eta\text{-C}_5\text{H}_5)$ ).<sup>40c</sup> The heterobimetallic complexes  $[(\text{PPh}_3)_2\text{HRe}(\mu\text{-H})_3(\mu\text{-CO})\text{Ru}(\eta^2\text{-H}_2)(\text{PPh}_3)_2]$  ( $T_{1\text{min}}$  10 ms at 213 K) and  $[(\text{PPh}_3)_2\text{HRe}(\mu\text{-H})(\mu\text{-Cl})_2(\mu\text{-CO})\text{Ru}(\eta^2\text{-H}_2)(\text{PPh}_3)_2]$  ( $T_{1\text{min}}$  9 ms at 213 K) have also been suggested to contain intact  $\text{H}_2$  ligands.<sup>40d</sup>

To verify that **8** is a catalyst precursor for the hydrogenation of acetylacetone and not a catalytically inactive side-product, a methanol solution of **8**, generated in situ as described above, was injected into an autoclave containing 80 equiv of acetylacetone. After pressurizing with 50 bar of  $\text{H}_2$ , the reactor was heated to 40 °C for 24 h. The conversion to (*R*)-(*R*)-2,4-pentanediol (95%) and the ee (87%) were practically identical with those observed for the analogous reaction promoted by the precursor **6a** (entry 2, Table 7).

Although one may not exclude that the deoligomerization of **8** takes place under hydrogenation conditions to give NMR-undetectable traces of a catalytically active mononuclear complex, the participation of a dimeric species in the catalysis cycle is very much likely indeed. In actuality, **8** represents a resting state which can easily generate a vacancy for the substrate by decoordination of labile  $\text{H}_2$  and also possesses the hydride groups for the reduction of the substrate. On the other hand, in comparable experimental conditions (Tables 6 and 7), the dimer **6a** and the monomer **7** exhibit quite different activity and enantioselectivity for the hydrogenation of acetylacetone, which suggests the action of distinct catalysts.

## Conclusions

The new optically pure  $C_1$ -symmetric diphosphine (*R*)-(*R*)-3-benzyl-2,4-bis(diphenylphosphino)pentane (BDPBzP) has been synthesized and used in combination with Ru(II) ions to catalyze the hydrogenation of acetylacetone to (*R*)-(*R*)-2,4-pentanediol with ee's up to 95%. The best catalytic performance is exhibited by a dimeric precursor of the formula  $[(\text{BDPBzP})(\text{DMSO})\text{Ru}(\mu\text{-Cl})_3\text{RuCl}(\text{BDPBzP})]$ . An in situ high-pressure NMR study

(39) (a) Bakmutov, V. I.; Vorontsov, E. V. *Inorg. Chem.* **1998**, *18*, 183. (b) Heinekey, D. M.; Warren, J. O., Jr. *Chem. Rev.* **1993**, *93*, 913. (c) Bakmutov, V. I.; Bianchini, C.; Maseras, F.; Lledos, A.; Peruzzini, M.; Vorontsov, E. V. *Chem. Eur. J.* **1999**, *5*, 3318.

(40) (a) Mezzetti, A.; Costella, L.; Del Zotto, A.; Rigo, P. *Gazz. Chim. Ital.* **1993**, *123*, 155. (b) Arliguie, T.; Chaudret, B.; Morris, R. H.; Sella, A. *Inorg. Chem.* **1988**, *27*, 598. (c) Hampton, C.; Cullen, W. R.; James, B. R. *J. Am. Chem. Soc.* **1988**, *110*, 6918. (d) Cazanoue, M.; He, Z.; Neibecker, D.; Mathieu, R. *J. Chem. Soc., Chem. Commun.* **1991**, 307.



in catalytic conditions has shown that the nonclassical polyhydride dimer  $[(\text{BDPBzP})(\eta^2\text{-H}_2)\text{ClRu}(\mu\text{-H})_2\text{RuCl}(\eta^2\text{-H}_2)(\text{BDPBzP})]$  (**8**) is the only species detectable on the NMR time scale all over the catalytic cycle. On the basis of in situ and reactor studies, it is proposed that no deoligomerization of the precursor occurs in the course of the catalysis.

Coordination of various transition metals, extension of the range of prochiral substrates, and prospects for heterogenization remain exciting results for the application of BDPBzP to asymmetric catalysis. Preliminary results in the hydrogenation and hydroboration of alkenes by rhodium catalysis and in the allylic alkyla-

tion of olefins by palladium catalysis show that BDPBzP gives rise to efficient enantioselective catalysts.

**Acknowledgment.** Thanks are due to MURST (legge 95/95) for financial support. Dante Masi is gratefully acknowledged for the technical assistance in the X-ray structure determination.

**Supporting Information Available:** Complete details of X-ray diffraction study on **5** and variable-temperature NMR spectra of **6a** (Figure S1). This material is available free of charge via the Internet at <http://pubs.acs.org>.

OM000137Y